Electronic Supplementary Material (ESI) for Dalton Transactions.

One-step synthesis of water-soluble hexagonal $NaScF_4$:Yb/Er nanocrystals with intense red emission

Min Pang, [a,b] Xuesong Zhai, [a] Jing Feng,*[a] Shuyan Song,[a] Ruiping Deng, [a] Zhuo Wang, [a,b] Shuang Yao,[a] Xin Ge [a] and Hongjie Zhang,*[a]

[a]State Key Laboratory of Rare Earth Resource Utilization, Changchun Institute of Applied Chemistry, Chinese Academy of Sciences, 5625 Renmin Street, Changchun 130022, China
[b]University of Chinese Academy of Sciences, Beijing, 100049, China

*Corresponding author

Email: fengj@ciac.jl.cn (Jing Feng); hongjie@ciac.jl.cn (Hongjie Zhang)

Tel: 86-431-85262127.

Fax: 86-431-85698041.

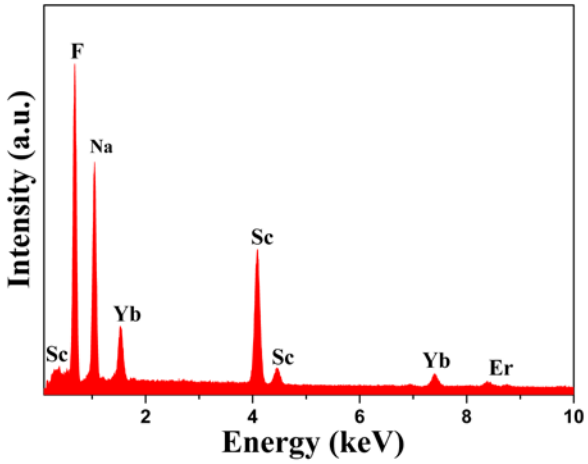

Fig. S1 EDS pattern of the as-synthesized $NaScF_4$:Yb/Er UCNCs.

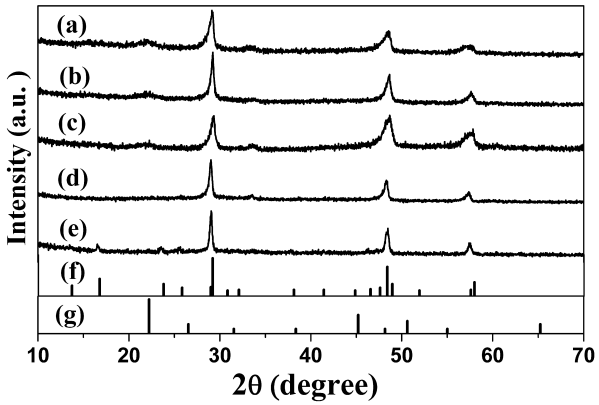

Fig. S2 XRD patterns of $NaScF_4$:Yb/Er NCs obtained at different reaction times (a) 30 min; (b) 1 h; (c) 1.5 h; (d) 2 h; (e) 4 h; the standard peaks of (f) hexagonal $NaScF_4$ and (g) orthorhombic ScF_3, respectively.

Fig. S2 shows the XRD patterns of the products prepared at different reaction times. The XRD patterns of the sample obtained at the initial stage (30 min) revealed the presence of impurities. The impure peaks at 2θ=22.2 degree mainly correspond to the orthorhombic ScF_3. When the reaction time extended, impure peaks gradually disappeared. The pure hexagonal phase ($NaScF_4$) was obtained at 2 h. The diffraction intensity became stronger as reaction time extended, indicating that crystallinity increased. Therefore, the time-dependent experiments demonstrated that hexagonal $NaScF_4$:Yb/Er NCs had been synthesized in 2 hours.

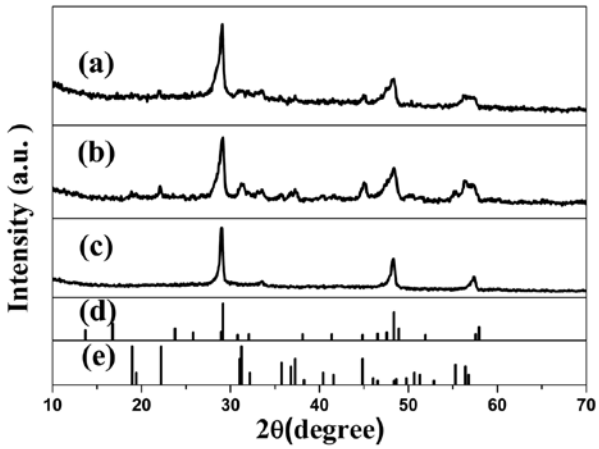

Fig. S3 XRD patterns of $Na_xScF_{3+x}:Yb^{3+}/Er^{3+}$ (20/2 mol %) UCNCs obtained under (a) Na:Sc=3:1 (b) Na:Sc=2:1 and (c) Na:Sc=1:1, the standard peaks in pure hexagonal $NaScF_4$ (d) and monoclinic (e) Na_3ScF_6 phases, respectively.

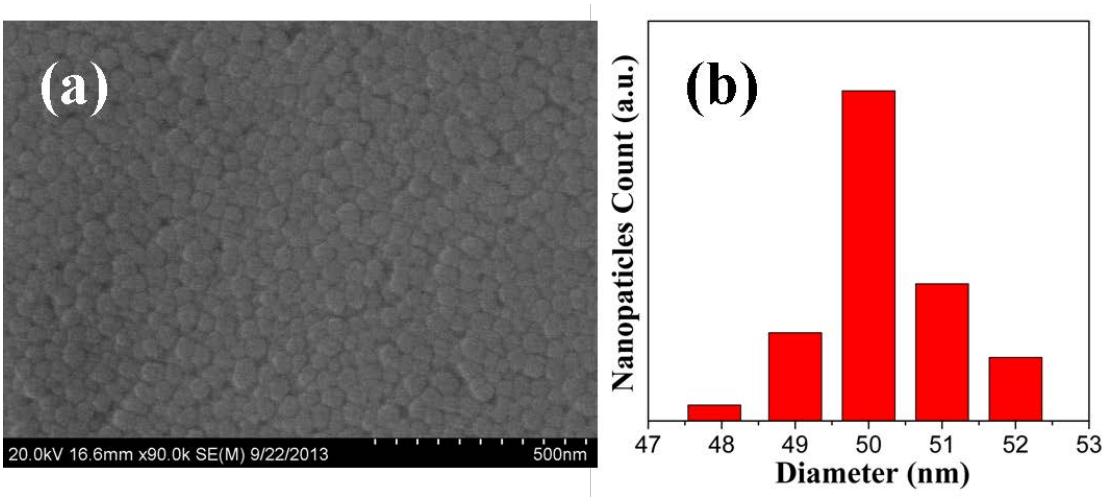

Fig. S4 (a) SEM image and (b) the corresponding histogram of $NaYF_4:Yb^{3+}/Er^{3+}$ (20/2 mol%) NCs. The particle size and dopant concentration of the $NaYF_4$ and $NaScF_4$ NCs were similar.

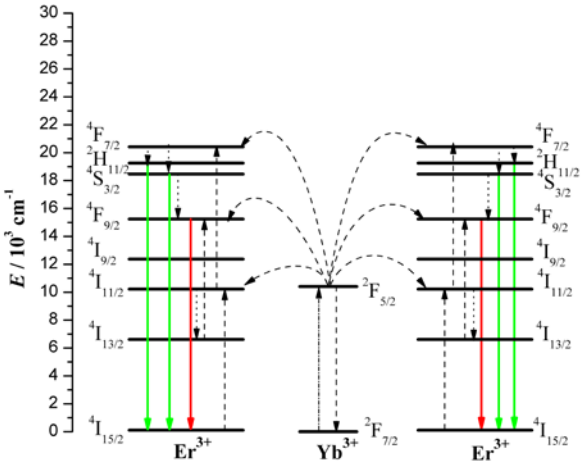

Fig. S5 UC energy transfer mechanisms of the as-prepared $NaScF_4$:Yb/Er UCNCs.

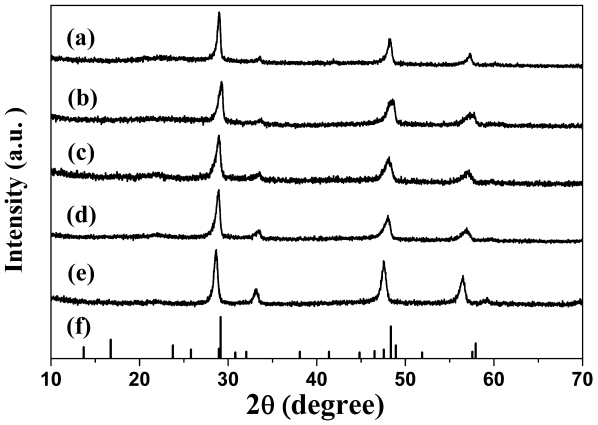

Fig. S6 XRD patterns of $NaScF_4$:Yb/Er (m/2 mol %) NCs doped with different Yb^{3+} ion concentrations (a) m= 20, (b) m = 30, (c) m = 40, (d) m = 50, (e) m = 60 and the standard peaks of hexagonal $NaScF_4$.

When $NaScF_4$:Er/Yb NCs doped with various level of Yb^{3+}, the XRD patterns (Fig. S6) match well with that of standard hexagonal structured $NaScF_4$. Compared with standard peaks of hexagonal $NaScF_4$, the slight shifts of the peaks were caused by the incorporation of Yb^{3+} ions into the $NaScF_4$ NCs.

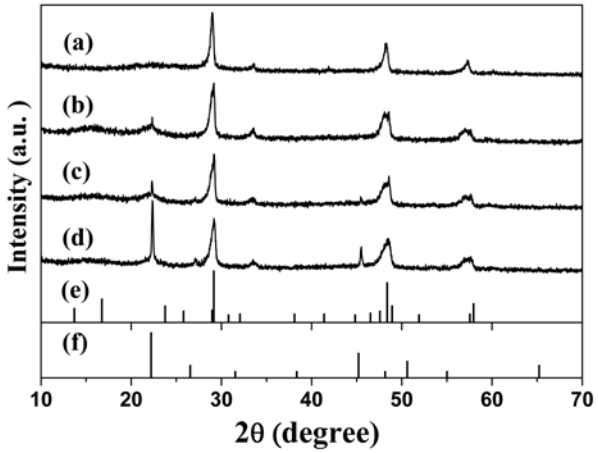

Fig. S7 XRD patterns of $NaScF_4$:Yb/Er (20/n mol %) NCs doped with different Er^{3+} ion concentrations (a) n = 2, (b) n = 4, (c) n = 6, (d) n = 8, the standard peaks of (e) hexagonal $NaScF_4$ and (f) orthorhombic ScF_3, respectively.

When the concentration of Er^{3+} ion extended to 4 mol % or more, impure peaks indexed to the orthorhombic ScF_3 would appear (Fig. S6). Therefore, the appropriate dopant concentrations of Er^{3+} is about 2 mol% in the system. No impure peaks occurred in $NaScF_4$:Er/Yb NCs when doping concentration of Yb^{3+} was gradually enhanced, which was probably because of the similar radius between Sc^{3+} and Yb^{3+} ions.

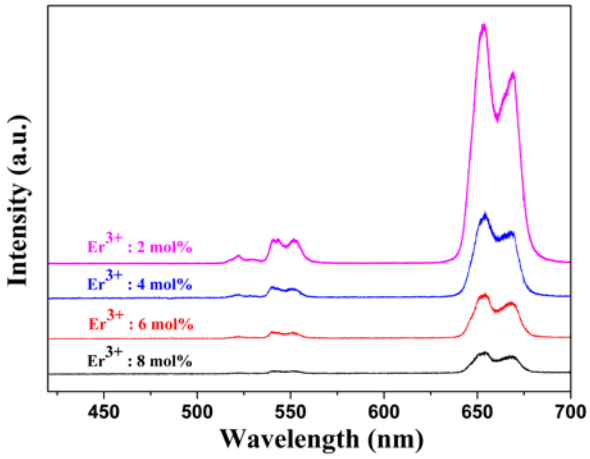

Fig. S8 UC luminescence spectra of $NaScF_4$:Yb/Er NCs doped with different Er^{3+} ion concentrations in the range of 2–8 mol%.

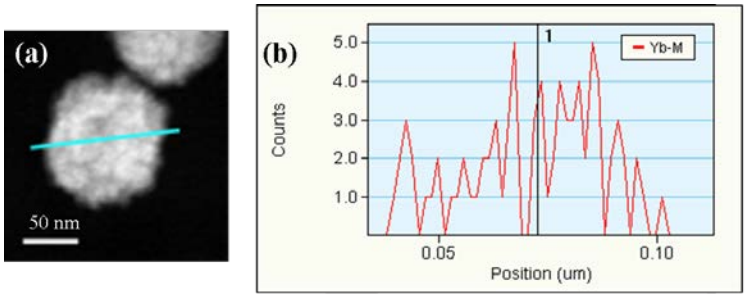

Fig. S9 STEM image of $NaScF_4$:Yb/Er (40/2%) @ $NaScF_4$:Yb (10%) NCs (a) and EDS line scan (b) showing the signal intensity variation of Yb across a randomly selected core–shell NCs. The Yb content at particle edge is lower than that in the interior, which is very consistent with the designed core–shell structure.